PHYSICAL REVIEW B **69**, 100506(R) (2004)

Identical superconducting gap on different Fermi surfaces of $Ca(Al_{0.5}Si_{0.5})_2$ with the AlB_2 structure

S. Tsuda,[1] T. Yokoya,[1] S. Shin,[1,2] M. Imai,[3] and I. Hase[4]

[1]*Institute for Solid State Physics, University of Tokyo, 5-1-5 Kashiwa-no-ha, Kashiwa, Chiba 277-8581, Japan*

[2]*The Institute of Physics and Chemical Research (RIKEN), 1-1-1 Kouto, Mikazukichou, Sayo-gun, Hyogo 660-0891, Japan*

[3]*National Institute for Material Science, 1-2-1 Sengen, Tsukuba, Ibaraki 305-0047, Japan*

[4]*Nanoelectronics Research Institute, National Institute of Advanced Industrial Science and Technology, 1-1-4 Umezono, Tsukuba, Ibaraki 305-8568, Japan*

(Received 6 October 2003; revised manuscript received 2 February 2004; published 30 March 2004)

Angle-resolved photoemission spectroscopy of $Ca(Al_{0.5}Si_{0.5})_2$ (CaAlSi), which is a superconductor (transition temperature is 7.7 K) with the AlB_2 structure, revealed that superconducting gaps on two Fermi surfaces (FSs) with three-dimensional character around $\Gamma(A)$ and $M(L)$ in the Brillouin zone provide essentially the same superconducting gap value (~ 1.2 meV± 0.2 meV). This is in contrast to the case of MgB_2, in which different FSs exhibit different gap values. The reduced gap value $2\Delta(0)/k_BT_c$ of $\sim 4.2 \pm 0.2$ classifies CaAlSi as a moderately strong-coupling superconductor.

DOI: 10.1103/PhysRevB.69.100506 PACS number(s): 74.70.Ad, 74.25.Jb, 74.20.Rp, 79.60.−i

After the discovery of an unexpectedly high-temperature superconductivity in MgB_2,[1] intensive studies of MgB_2, as well as related compounds, have been performed to understand the mechanism of its superconductivity.[2] From the magnitude and symmetry of the superconducting (SC) gap, which are closely related to the strength and origin of the driving force of the Cooper pair, respectively, evidence for an unusual SC gap and not a simple isotropic *s*-wave gap have been concluded.[2] The unusual gap has been explained in terms of a multiple gap scenario,[3] which predicts two gaps with different magnitudes originating in two Fermi-surface (FS) sheets with different symmetry. Although the relationship between the gaps and the character of FSs has been addressed using tunneling spectroscopy[4] and Raman spectroscopy,[5] more recently, direct evidence for an unusual SC gap has been provided by angle-resolved photoemission spectroscopy (ARPES).[6,7] ARPES has the capability of detecting momentum (k)-resolved electronic structures and, hence, could confirm k dependence of a SC gap in MgB_2. These ARPES studies have clarified a larger gap on the two-dimensional (2D) FS sheet derived from the σ orbital and a smaller gap on the three-dimensional (3D) FS derived from the π orbital, showing two-band superconductivity as an origin for both the unusual SC gap and the high transition temperature (T_c). In comparison, ARPES studies of the SC gap in related compounds which possess the same structure have not been reported so far, since superconductivity of the compounds with the AlB_2 structure has not been reliably obtained and/or the T_c is too low to be accessed by ARPES measurements due to instrumental limitations of sample cooling. This may leave a question whether such an unusual SC gap is a characteristic of MgB_2.

$Ca(Al_{0.5}Si_{0.5})_2$ (CaAlSi) is isostructural with MgB_2 and shows superconductivity below 7.7 K,[8,9] which is, to our knowledge, the highest T_c in ternary compounds having the AlB_2 structure. Furthermore, band-structure calculations[10] have predicted that CaAlSi has two FS sheets, both of which have 3D character. This is in contrast to MgB_2, which exhibits two types of FS sheets, consisting of a 2D σ-derived FS and a π-derived 3D FS. Since, in MgB_2, the SC gap values depend on the characters of the FS sheets, in the comparison between CaAlSi and MgB_2 it is interesting to see the peculiarity of the electronic structure of MgB_2.

In this paper we report on the ARPES results on the band dispersion and the FS dependence of the SC gap of CaAlSi. The valence-band ARPES study of CaAlSi shows fairly good agreement with band-structure calculations, except for one band that can be ascribed to a surface-state band. The SC gaps on different FS sheets, both with 3D character, are found to be nearly of the same magnitude of ~ 1.2 meV ± 0.2 meV, resulting in a reduced gap value of $\sim 4.2 \pm 0.2$. This is, to our knowledge, the first data reporting a FS sheet-dependent measurement of the SC gap of MgB_2 related compounds. This result provides important insights to the role of the character of the FS for the superconducting properties of AlB_2-type compounds.

The CaAlSi single crystals were synthesized by a floating-zone method. The details were described in Ref. 11. X-ray diffraction measurements confirmed that our CaAlSi single crystals have the AlB_2 crystal structure with lattice constants $a = 4.19002(3)$ Å and $c = 4.3978(6)$ Å, as reported earlier.[8,11] Sample orientations were identified by Laue backscattering measurements performed *ex situ* and further confirmed by the symmetry of ARPES spectra. All the ARPES spectra were obtained with a high-resolution hemispherical analyzer using monochromatic He resonance lines [He Iα (21.218 eV) and He IIα (40.814 eV)]. ARPES valence-band spectra were taken with $a \sim 30$ meV energy resolution and ultrahigh-resolution spectra for SC gaps were taken with a 3.1 meV resolution. The instrumental angular resolution was set to $\pm 0.2°$. The samples were cleaved and measured *in situ* under an ultrahigh vacuum condition with a base pressure better than 5×10^{-11} Torr. The binding energy (BE) and the energy resolution of each spectrum were calibrated with the Fermi edge of a gold film evaporated onto a copper substrate near the samples. The accuracy of the Fermi energy (E_F) is better than 5 meV for valence-band measurements and 0.2 meV for SC gap measurements.

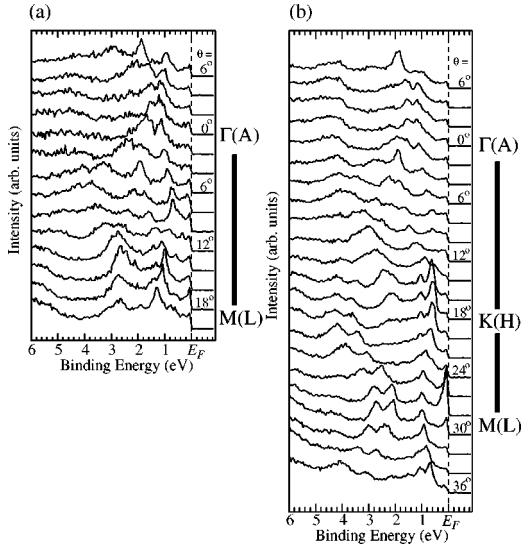

FIG. 1. The valence-band ARPES spectra of CaAlSi obtained with He IIα measured along the (a) $\Gamma(A)$-$M(L)$ and (b) $\Gamma(A)$-$K(H)$-$M(L)$ high symmetry directions.

We also calculated the band structure of CaAlSi with the standard full-potential augmented plane-wave (FLAPW) method, in order to identify the character and dimensionality of each FS sheet observed experimentally. We have carried out this calculation by using the computer code KANSAI-94 and TSPACE.[12] For the exchange-correlation potential we adopted the local-density approximation (LDA), according to Gunnarson and Lundqvist.[13] The calculation of the core states and the valence states are self-consistently carried out by the scalar-relativistic scheme.[14] We used the experimentally known lattice constants and space group.[8,11] The muffin-tin radius of each atom is 0.38a for Ca, 0.23a for Al and Si. The basis functions with the wave vector $|k+G| < K_{\max}=3.6(2\pi/a)$, where k is a wave vector in the Brillouin zone (BZ) and G is a reciprocal-lattice vector, resulting in about 270 basis linear augmented plane waves (LAPWs).

Figure 1 shows ARPES spectra from a CaAlSi(0001) cleaved surface measured along the (a) $\Gamma(A)$-$M(L)$ and (b) $\Gamma(A)$-$K(H)$-$M(L)$ high symmetry directions in the BZ with the He IIα resonance line. Here, we only discuss the overall valence-band dispersions with He IIα, because the background coming from secondary electrons is much lower and the accessible BE and reciprocal space are much wider in He IIα than in He Iα. In Fig. 1, ARPES spectra have several peaks whose intensity and energy position systematically change as a function of the measured k. As for the structure near E_F, one can see an intense peak structure around $M(L)$, which appears to form an electron pocket. To make the band dispersions more visible, we took a second derivative of the raw spectra shown in Fig. 1 and plotted the intensity as a function of BE and k, as shown in Fig. 2. Higher intensity regions plotted with yellow (and red for much higher intensity region) correspond to electronic bands. We observed several dispersive bands within 6 eV of E_F having the same periodicity as that of the bulk BZ, especially for the $\Gamma(A)$-$K(H)$-$M(L)$ line. Near E_F, besides the highest intensity region around the $M(L)$ point that is evident from the raw data, we also find that higher intensity regions exist around the $\Gamma(A)$ point and at halfway of both, $\Gamma(A)$-$K(H)$ and $\Gamma(A)$-$M(L)$. We also observe two higher intensity re-

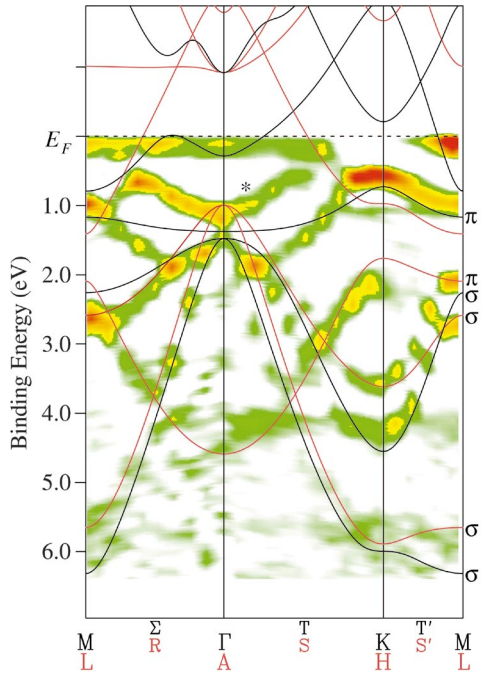

FIG. 2. (Color) The second-derivative valence-band intensity map of CaAlSi along the $\Gamma(A)$-$M(L)$ and $\Gamma(A)$-$K(H)$-$M(L)$ directions. The higher intensity regions correspond to the bands. The curves show the calculated band dispersions with the FLAPW method; the black and red curves represent the dispersion on $k_z=0$ and π/c planes in the BZ, respectively.

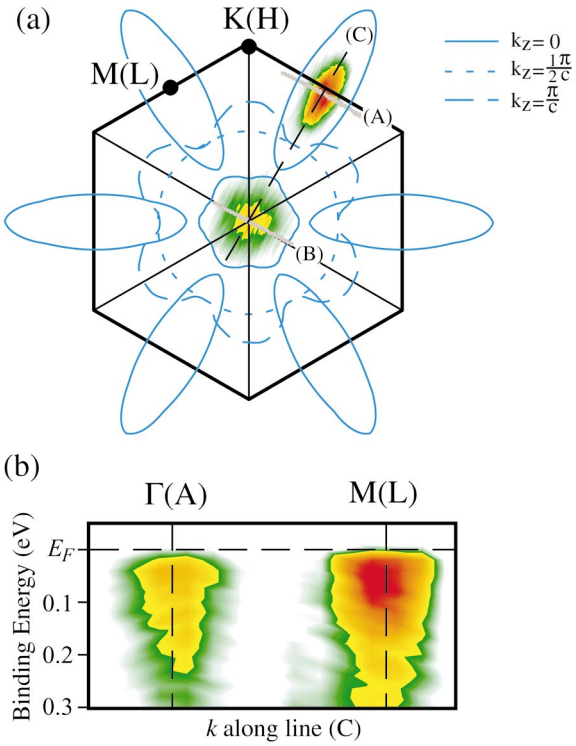

FIG. 3. (Color) (a) The FS map of CaAlSi. Each blue curve shows calculated FSs on different k_z planes (see text). (b) The intensity map of CaAlSi along the line (C) of (a) corresponding to the Γ-M line.

gions near E_F around the $\Gamma(A)$ and $M(L)$ points along $\Gamma(A)$-$M(L)$, which suggest the existence of electronlike FS sheets. This is consistent with the Hall coefficient measurements reporting that the dominant carriers in CaAlSi are electrons.[11]

The black and red curves superimposed in Fig. 2d correspond to the calculated band dispersions as a function of BE and k on the $k_z=0$ and π/c planes, respectively. The calculated energy-band structure is in good agreement with the previous report.[10] The characters of selected bands are indicated at the right side of the figure with "σ" and "π." The σ bands are composed mainly of the $3s$, $3p_x$, and $3p_y$ electrons of Al and Si, while the π bands are composed mainly of $3p_z$ electrons of Al and Si. The rest of the bands originate from highly hybridized 3D electronic states of Ca, Al, and Si. The calculated band dispersions for the σ and π bands located from 1.5 to 6.0 eV appear very similar to the experimental dispersions, though a larger deviation is observed for the π band from $k_z=0$ plane around the Γ point.[15] Simultaneous observation of two bands from $k_z=0$ and π/c may be due to k_z broadening, which originates from a smaller escape depth of photoelectrons due to a band gap in the final state or due to the photon energy used (He IIα).[16] We can also find that the observed features near E_F have a similarity to the calculated band dispersions. The electron pocketlike structure at $M(L)$ corresponds to the 3D band at $k_z=0$, though the energy position of the calculated-band bottom has higher BE compared with the experimental-band bottom. This shift of the band bottom may be caused by a narrowing of the bandwidth in consideration with the observation of another electron pocketlike structure at $\Gamma(A)$, which can also be related to the 3D band at $k_z=0$. The features located halfway along $\Gamma(A)$-$M(L)$ and $\Gamma(A)$-$K(H)$ can be assigned to the 3D band at $k_z=\pi/c$. Thus we can assign the band dispersions near E_F to the 3D bands from different k_z planes. An important finding from the valence-band study is that CaAlSi has 3D FS sheets only. We found that another band around 1 eV, indicated with an asterisk, cannot be assigned to any calculated bands. We attribute this $\star$ band to a surface state, as we found that structure degraded very rapidly when the air was introduced into the measurement chamber. A similar surface state band around $\Gamma(A)$ was also reported in MgB_2.[17]

Next, we discuss the electronic structure near E_F with the data obtained with the He Iα resonance line, because higher intensity of He Iα makes it possible to study band structures near E_F in more detail. It is also possible to measure the SC gap with the higher resolution, as compared with He IIα. In Fig. 3 we plotted spectral intensities around E_F with a 40 meV energy window over the BZ (the thick hexagon indicates the first BZ). Higher intensity regions plotted with yellow (and red for much higher intensity region) correspond to FSs. Figure 3(b) is the spectral intensity map as a function of BE and k along the thin broken line (C) of Fig. 3(a). We used different color scales in Figs. 3(a) and 3(b) to emphasize the FSs and the bands. In Fig. 3(b), the two electron pocketlike structures around $\Gamma(A)$ and $M(L)$ are more clearly seen than in Fig. 1 or 2. This is most probably due to higher signal-to-noise ratio and the longer escape depth of photoelectrons using He Iα compared to He IIα, leading to better identification of k_z values. In Fig. 3(a) these structures form a hexagonal-like and an elliptical intensity distribution around $\Gamma(A)$ and $M(L)$, respectively. As mentioned above, both FSs are 3D, hence we compared with the calculated FSs at different k_z planes in Fig. 3(a) by blue curves, where the solid, dotted, and broken curves correspond to the intersections of two FSs (one is a pancakelike FS around Γ and the other is a sixfolded gearlike FS centered at Γ that has six ellipsoidal holes around M along k_z) on $k_z=0$, $\pi/2c$, and π/c, respectively. As seen in Fig. 3(a), the two FSs observed with He Iα show good correspondence to FS sheets at $k_z=0$. The negligible intensity around the midpoints along $\Gamma(A)$-$M(L)$ and $\Gamma(A)$-$K(L)$, which are observed using He Iα, suggests that we dominantly detected electronic structures near E_F from $k_z\sim 0$ using He Iα.

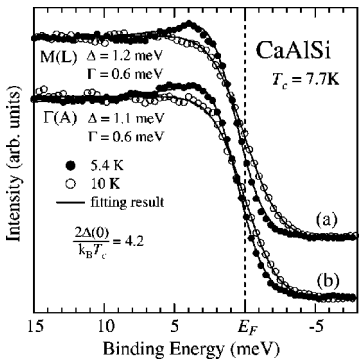

FIG. 4. Temperature-dependent ultrahigh-resolution spectra of CaAlSi measured on the FS sheets at the $M(L)$ and $\Gamma(A)$ points. The open and filled circles show the experimental spectra of the normal and the SC states, respectively (see text).

Figure 4 shows ultrahigh-resolution (3.1 meV) temperature-dependent spectra in the vicinity of E_F measured on the gearlike sheet along line (A) in Fig. 3 and the pancakelike FS sheet along line (B) are shown in Fig. 4. To compensate the low count rate owing to the higher resolution used, the spectra shown in Fig. 4 are the sum of ARPES spectra along the two lines, representing a nearly one-dimensional density of states. This allows us to do a Dynes function analysis (below), which was originally used for describing the superconducting density of states. The open and filled circles represent the experimental results measured at 5.4 K (normal) and 10 K (SC), respectively. Below T_c of 7.7 K, we observe a midpoint shift of the leading edge and a quasiparticle peak around 4 meV BE, indicative of opening of the SC gap for both FS sheets. To estimate the magnitude of the SC gaps (Δ), we fit the data with the Dynes function,[18] including a broadening parameter Γ.[19] A Dynes function was first multiplied with a Fermi-Dirac function of the measured temperature and then convoluted with a Gaussian with a full width at half maximum (FWHM) equal to the experimental resolution.[20] We determine Δ's and Γ's so that the observed spectra can be well reproduced with the calculated spectra as seen for the peak and the leading edge regions. The solid curves in Fig. 4 are the fitting results. The Δ values for the FS around $\Gamma(A)$ and $M(L)$ are 1.1 and 1.2 meV, respectively, which indicates that the SC gaps are of the same magnitude within the accuracy of the fitting process $zx<(\pm 0.2$ meV).[21] We estimated the gap values at 0 K from

the known temperature dependence of the SC gap[22] and obtained 1.4 ± 0.1 meV. The reduced gap value $2\Delta(T=0\ \mathrm{K})/k_BT_c$ is 4.2 ± 0.2, which is larger than the BCS value of 3.52, classifying CaAlSi as a moderately strong-coupling superconductor. As for the Γ, we needed a relatively large value (0.6 meV) compared to Δ. One possible reason for that is an anisotropy in the k_z direction, consistent with magnetization measurements.[11,23] On the other hand, the chance that an in-plane gap anisotropy can be eliminated from magnetization measurements[11,23] is reported when the in-plane anisotropy is negligible.

Thus, the present results in CaAlSi are in sharp contrast to the multiple gaps observed in MgB_2. In MgB_2, the two gaps with different magnitude open on the two FS sheets with very different characters (2D σ band and 3D π band). On the other hand, in CaAlSi, we observed identical gap value on different FS sheets with the same character (highly hybridized 3D electronic states of Ca, Al, and Si). Moreover, the reduced gap of 4.2 in CaAlSi is slightly larger than that for the larger gap in MgB_2 [3.56 (Ref. 6), 3.54 (Ref. 24)], suggesting that strong coupling is not required for explaining the T_c of MgB_2. Thus SC gap measurements on the different FS sheets of CaAlSi contrast the characteristic superconducting electronic structure of MgB_2 originating from the coexistence of FS sheets with different dimensionality. First-principle calculations[3] showed that, in MgB_2, the 2D FSs, or 2D bands can selectively couple to the high-frequency 2D phonon mode through k-dependent electron-phonon coupling. Thus MgB_2 is different from superconductors where k-dependent electron-phonon coupling does not play a major role, as in CaAlSi.[10]

In summary, we have performed ARPES of CaAlSi, which is a superconductor ($T_c=7.7$ K) with the AlB_2 structure. The experimental valence bands agree fairly well with the calculated results, except for a band that can be ascribed to a surface state. Measurements of the superconducting gap on the two different electron pockets around $\Gamma(A)$ and $M(L)$ in the BZ provide essentially the same superconducting gap value (~1.2 meV±0.2 meV), corresponding to the reduced gap value $2\Delta(0)/k_BT_c$ of $\sim4.2\pm0.2$. This indicates that CaAlSi is a moderately strong-coupling superconductor. Moreover, observed similar gap values on different FSs in CaAlSi, but with the same 3D character, contrast with the different gap values on different FSs in MgB_2, providing important insights to the role of dimensionality and symmetry for the superconducting properties of AlB_2-type compounds.

This work was supported by Grant-in-aid from the Ministry of Education, Science, and Culture of Japan. S.T. thanks the Japan Society for the Promotion of Science for financial support. We thank Professor A. Chainani for valuable discussions and a reading of the manuscript.

[1] J. Nagamatsu *et al.*, Nature (London) **410**, 63 (2001).
[2] C. Buzea and T. Yamashita, Supercond. Sci. Technol. **14**, R115 (2001).
[3] A. Y. Liu *et al.*, Phys. Rev. Lett. **87**, 087005 (2001); H. J. Choi *et al.*, Nature (London) **418**, 758 (2002); Phys. Rev. B **66**, 020513 (2002).
[4] R. S. Gonnelli *et al.*, Phys. Rev. Lett. **89**, 247004 (2002); M. Iavarone *et al.*, *ibid.* **89**, 187002 (2002); F. Giubileo *et al.*, *ibid.* **87**, 177008 (2001); Y. G. Naidyuk *et al.*, JETP Lett. **75**, 238 (2002); P. Martinez-Samper *et al.*, Physica C **385**, 233 (2003); M. R. Eskildsen *et al.*, *ibid.* **385**, 169 (2003).
[5] J. W. Quilty *et al.*, Phys. Rev. Lett. **90**, 207006 (2003).
[6] S. Tsuda *et al.*, Phys. Rev. Lett. **91**, 127001 (2003).
[7] S. Souma *et al.*, Nature (London) **423**, 65 (2003).
[8] M. Imai *et al.*, Appl. Phys. Lett. **80**, 1019 (2002).
[9] M. Imai *et al.*, Physica C **377**, 96 (2002); M. Imai *et al.*, *ibid.* **382**, 361 (2002).
[10] I. R. Shein *et al.*, JETP Lett. **76**, 189 (2002).
[11] M. Imai *et al.*, Phys. Rev. B **68**, 064512 (2003).
[12] A. Yanase, *Fortran Program For Space Group (TSPACE)* (Shokabo, Tokyo, 1995) (in Japanese).
[13] O. Gunnarson and B. I. Lundqvist, Phys. Rev. B **13**, 4274 (1976).
[14] D. D. Koelling and B. N. Harmon, J. Phys. C **9**, 3107 (1977).
[15] The band has a dispersion matching with the bulk periodicity and shows different behavior compared to the band "*" (discussed later) for the air exposed surface. This fact confirms the bulk origin of the band. It may be plausible to think that effects not taken into consideration in the calculations may induce the difference. For example, while the calculation is performed for the system with ordered Al and Si atoms, Al and Si atoms are located at random, but equivalent, sites in a real crystal.
[16] P. J. Feibelman and D. E. Eastman, Phys. Rev. B **10**, 4932 (1974).
[17] H. Uchiyama *et al.*, Phys. Rev. Lett. **88**, 157002 (2002).
[18] R. C. Dynes *et al.*, Phys. Rev. Lett. **41**, 1509 (1965).
[19] The Γ is used originally for explaining the lifetime broadening of quasiparticles in SC states (Ref. 18), but is usually taken as a fitting parameter reflecting other information on sample quality, k dependence of a SC gap, and so forth, as well as the lifetime broadening.
[20] A detailed dispersion of a band crossing E_F will affect the k-integrated spectral shape near E_F. This effect can normally be taken into consideration by multiplying a polynomial to a Dynes function. In the present case, we did not use any polynomial for both the spectra because we found that the normal state density of states are constant within the very small energy window from 15 meV binding energy to 5 meV above E_F.
[21] Obtained Δ and Γ values are smaller compared to the resolution we used (3.1 meV). However, the resolution we refer to (3.1 meV) is the resolving power for closely located two peaks and is different from the resolution or accuracy for determining an energy position. The energy-position resolution, which is what we need for determining Δ and Γ values, is more than 10 times higher than the resolving-power resolution.
[22] D. J. Scalapino, in *Superconductivity*, edited by R. D. Parks (Dekker, New York, 1969), Vol. 1, Sec. IV.
[23] T. Tamegai *et al.*, J. Low Temp. Phys. **131**, 1153 (2003); A. K. Ghosh *et al.*, Phys. Rev. B **68**, 054507 (2003).
[24] S. Tsuda *et al.*, Phys. Rev. Lett. **87**, 177006 (2001).